

Report No. IITRI-A6141-FR1
(Final Report)

A HIGH ALTITUDE MEASUREMENT TO DETERMINE
THE RATIO OF DEUTERIUM TO HYDROGEN IN THE
SOLAR ATMOSPHERE

National Aeronautics & Space Administration
Office of Space Science and Applications
Washington, D.C. 20546

IIT RESEARCH INSTITUTE

Report No. IITRI-A6141-FR1
(Final Report)

A HIGH ALTITUDE MEASUREMENT TO DETERMINE THE RATIO OF
DEUTERIUM TO HYDROGEN IN THE SOLAR ATMOSPHERE

1 June 1965 to 30 March 1966

Prepared by
Dr. Gordon Henderson

of

IIT RESEARCH INSTITUTE
Technology Center
Chicago, Illinois 60616

for

National Aeronautics and Space Administration
Office of Space Science and Applications
Washington, D.C. 20546
Attention: Dr. Harold Glaser

IIT RESEARCH INSTITUTE

FOREWORD

This report is the final report on NASA Contract No. NASr 65(13)/14-003-913 which is a preliminary phase of an experiment to attempt the detection of deuterium in the solar photosphere by accurately recording the profiles of the H_{α} and H_{β} Fraunhofer lines.

The work carried out has been directed to the realization of a system capable of achieving the required accuracy and still small enough to be installed in a high flying aircraft or balloon package.

The staff of IIT Research Institute appreciates the opportunity of conducting this research in the interest of advancing the state of the art in observational methods in solar physics.

Respectfully submitted,
IIT RESEARCH INSTITUTE



Gordon Henderson
Research Physicist
Optics Research

Approved by:



C. W. Terrell
Director
Physics Research

GH:sf

IIT RESEARCH INSTITUTE

N66-39493

ABSTRACT

Two optical systems have been investigated, each of which showed potential capability of providing a system capable of measuring the D/H ratio in the sun's atmosphere by observing the H_{α} Fraunhofer line. These were:

(i) An optical system consisting of a pair of Fabry-Perot interferometers in series which are scanned coherently. The interferometers are preceded by a narrow band interference filter.

(ii) An optical system consisting of a single Fabry-Perot interferometer in series with a scanning monochromator of the grating type. The interferometer and monochromator are scanned coherently.

Author

I. INTRODUCTION

In order to improve on attempts made to date on the problem of the existence of solar deuterium, two main goals must be achieved:-

- (i) An improvement in the accuracy of the measuring system.
- (ii) The removal of the cloaking effect of telluric water vapor absorption lines in the wings of the H_{α} profile.

To achieve the first goal, the use of photoelectric detectors is required. The detection system should have a digitized output and be automatically compensated for variations in atmospheric transmission. Moreover, the electronic amplification system should have an accuracy of 1 part in 10^4 and be compensated for long term drift to the same accuracy. Concomitant with the accuracy requirement is that of wavelength specification to the same order of accuracy as that of the signal measurement, i.e. 1 part in 10^4 . The second goal imposed the constraint on a system design that the instrumentation must be of such weight and dimensions that it can be installed in an aircraft or balloon.

The application of the Fabry-Perot interferometer to absorption spectroscopy entails a special problem which does not occur in emission spectroscopy. This problem related to the suppression of unwanted contributions to the measured signal

IIT RESEARCH INSTITUTE

from the continuum in the neighborhood of the absorption line under study. Two approaches to achieve this suppression are, (a) the use of a filter and a second Fabry-Perot in tandem with the first and, (b) the use of a grating monochromator operating at low resolution to limit the spectral region under study. Each of the above mentioned approaches has been evaluated in the present program to find which would be the better for the solar deuterium measurement. Method (b) appears to be more amenable to practical achievement. However, because of the potential of method (a) for high resolution absorption spectroscopy in general, this method should be further developed. Briefly, the main advantage of the multiple interferometer system is due to the much higher luminosity-resolving power product of the Fabry-Perot interferometer compared to any other dispersive system. In this respect the development of a multiple Fabry-Perot interferometer system employing magnetostrictive scanning will provide an important technique for high resolution absorption spectroscopy at low light levels.

II. OPTICAL SYSTEMS STUDY

A. Double Fabry-Perot Interferometer System

A study of the off-band suppression available with various combinations of Fabry-Perot interferometers and forefilters resulted in a decision to design the system to comprise:

IIT RESEARCH INSTITUTE

- (a) A 10A halfwidth forefilter centered on H_{α} at 6562.8A;
- (b) A scanning Fabry-Perot interferometer of 6A Free Spectral Range and a finesse of 30, giving a resolution of 0.2A;
- (c) A second scanning Fabry-Perot interferometer of 13.75A Free Spectral Range and a finesse of 30, giving a resolution of 0.46A.

When used in tandem these interferometers have an effective instrumental function given by

$$I = \left[\frac{T_1^2}{(1-R_1)^2} \right] \left[\frac{T_2^2}{(1-R_2)^2} \right] \left[\frac{1}{(1+F_1 \sin^2 \sigma_1/2) (1+F_2 \sin^2 \sigma_2/2)} \right]$$

where T_1, T_2 are the respective transmissions,

R_1, R_2 are the respective reflectances of the interferometer plates, and

F_1, F_2 are the respective finesses of the interferometers.

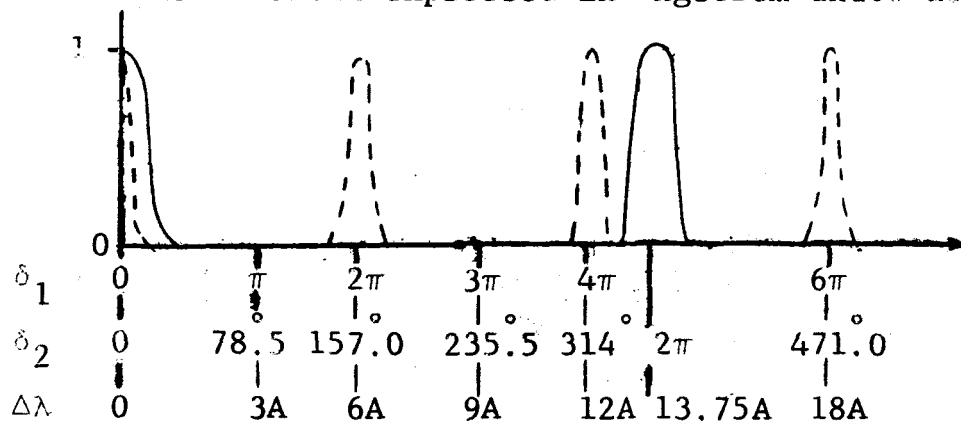
Table 1 below shows the relative magnitude of the interferometer combination for several selected order intervals.

Table 1. Transmittance Function for Two Fabry-Perot Interferometers

		A		B	
$\Delta\lambda$	δ_1	$(1+F_1 \sin^2 \delta_1/2)$	δ_2	$(1+F_2 \sin^2 \delta_2/2)$	$\frac{1}{AB}$
3A	π	2.4×10^3	78.5	9.8×10^2	4.25×10^{-7}
6A	2π	1	157.0	2.3×10^3	4.35×10^{-4}
9A	3π	2.4×10^3	235.5	2.04×10^3	2.08×10^{-7}
12A	4π	1	314.0	3.66×10^2	2.74×10^{-3}
18A	6π	1	471.0	1.63×10^3	6.14×10^{-4}

$\frac{1}{AB}$ gives the transmission of the combination relative to the maximum transmission at the common peak wavelength.

$\Delta\lambda$ is the interval expressed in Angstrom units as shown below:



When the instrumental function of the combination is combined with the narrow pass forefilter, the result is the overall transmission of the complete system. Table 2 shows the resulting system instrumental function. $T(\Delta\lambda)$ is the normalized transmission of the forefilter whose halfwidth is $10A$.

Table 2. Transmittance Function for Two Interferometers and a Forefilter of Halfwidth $10A$

$\Delta\lambda$	$\frac{1}{AB}$	$T(\Delta\lambda)$	$\frac{1}{AB} T(\Delta\lambda)$
3A	4.25×10^{-7}	0.81	3.4×10^{-7}
6A	4.35×10^{-4}	0.38	1.65×10^{-4}
9A	2.08×10^{-7}	0.10	2.08×10^{-8}
12A	2.74×10^{-3}	0.03	8.2×10^{-5}
18A	6.14×10^{-4}	0.008	4.9×10^{-5}

When two or more Fabry-Perot interferometers are used in tandem, there exist spurious maxima, or "ghosts" in the intensity pattern due to reflections between parallel faces of

the different interferometers. This so-called coupling and its prevention have been treated in detail recently by J. Schwider (Entkopplungsmöglichkeiten von Fabry-Perot Interferometern; Optica Acta, Vol. 12, No. 1, p.65, Jan 1965). The method employed in this work is somewhat similar to that of Geusic and Scovil referred to by Schwider. Figure 1 shows the arrangement used. With the method of scanning employed in this work, viz. magnetostriction, a problem arose in that it was difficult to maintain the transmission peaks of the two interferometers exactly in alignment. This problem was investigated and an apparently promising solution was tried. This consisted of using a common linear ramp generator for the two interferometers, followed by two low noise feedback amplifiers, one for each interferometer. The feedback resistor in each amplifier was replaced by a temperature compensated strain gauge placed across the interferometer gap so that any tendency for the spacing change between the plates to depart from linearity was counteracted by the negative feedback effect. Possible sources of non-linearity are thermal drifts and non-linearity of the magnetostrictive coefficient. Figure 2 shows a schematic representation of the electronic control system.

Figure 3 shows a photograph of one interferometer with a gauge in position. The adjacent gauge is one of the temperature compensating gauges.

The arrangement of a pair of Fabry-Perot interferometers is shown in Fig. 4 and a photograph of the system is shown in Fig. 5.

IIT RESEARCH INSTITUTE

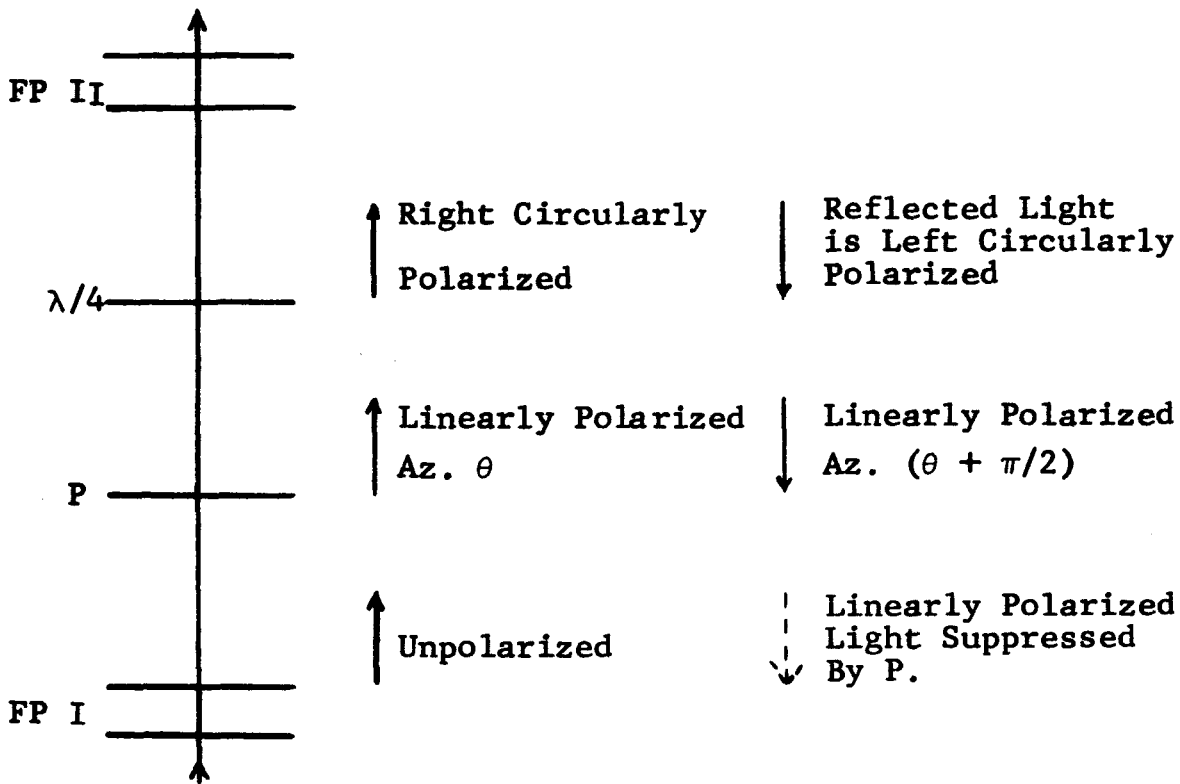


Figure 1, showing arrangement used to prevent coupling between Fabry-Perot interferometers in tandem.

ELECTRICAL BLOCK DIAGRAM FOR 2 INTERFEROMETER SYSTEM

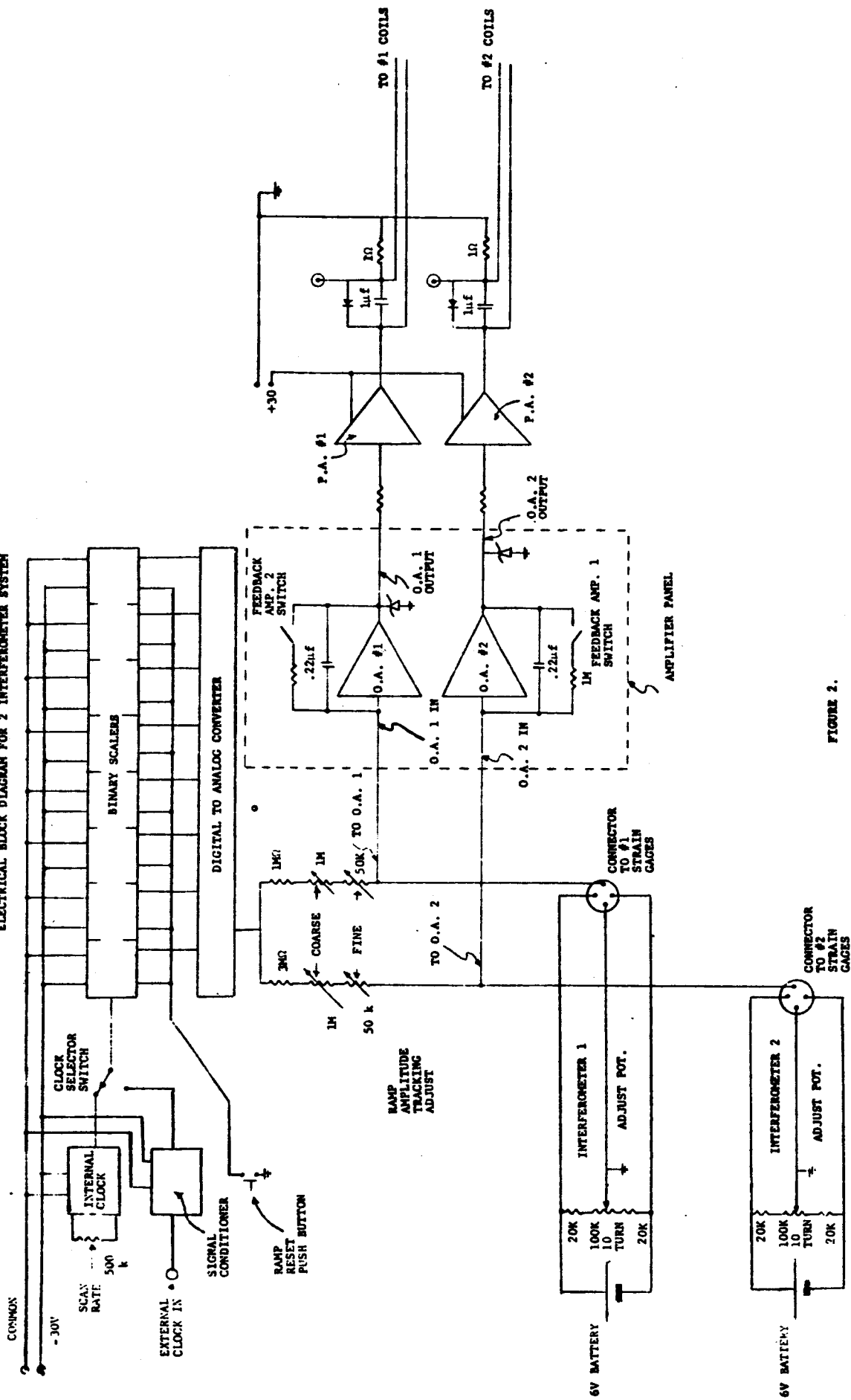


FIGURE 2.

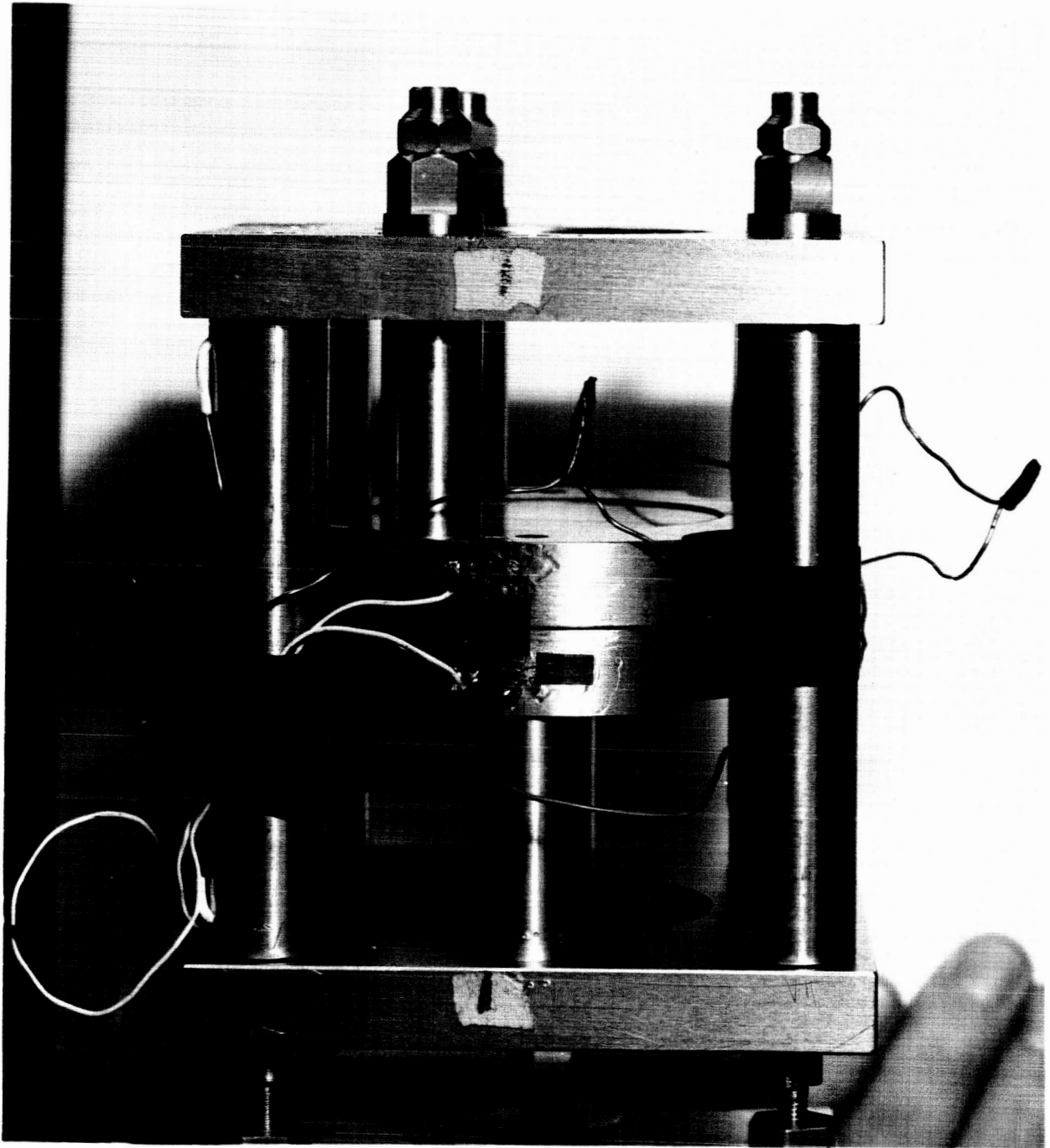


FIG. 3 PHOTOGRAPH OF STRAIN GAUGES FOR CONTROLLING SCAN OF PRISM INSTRUMENT

A difficulty experienced with the control system was the amount of thermal drift which the system suffered. The design of the strain gauge bridge attempted to compensate for thermal effects by placing a thermal compensating gauge adjacent to each active gauge, the compensating gauges making up the complete bridge circuit together with the active gauges. This arrangement however did not succeed in eliminating thermal drift completely and further work on the system was stopped in order to evaluate the alternative system described below.

B. Fabry-Perot Interferometer and Grating Monochromator

A sketch of the optical arrangement is shown in Fig. 6, and Fig. 7 shows a photograph of a breadboard model of the actual system. Synchronous scanning was achieved by connecting the scanning motor of the monochromator to the ramp generator which controls the scanning rate of the Fabry-Perot Interferometer. The monochromator is a Jarrell Ash 1/2 meter Ebert type instrument. Fig. 8 shows a block diagram of the electronic control system. The scanning motor of the monochromator was connected to the potentiometer by appropriate gearing, and the output of the potentiometer was used as the control signal for the interferometer system. The potentiometer output replaces the ramp generated by the scalars in the control system described in Fig. 2.

The optical performance of the system is illustrated in Figs. 9a-9d. Figure 9a shows the intensity distribution from a

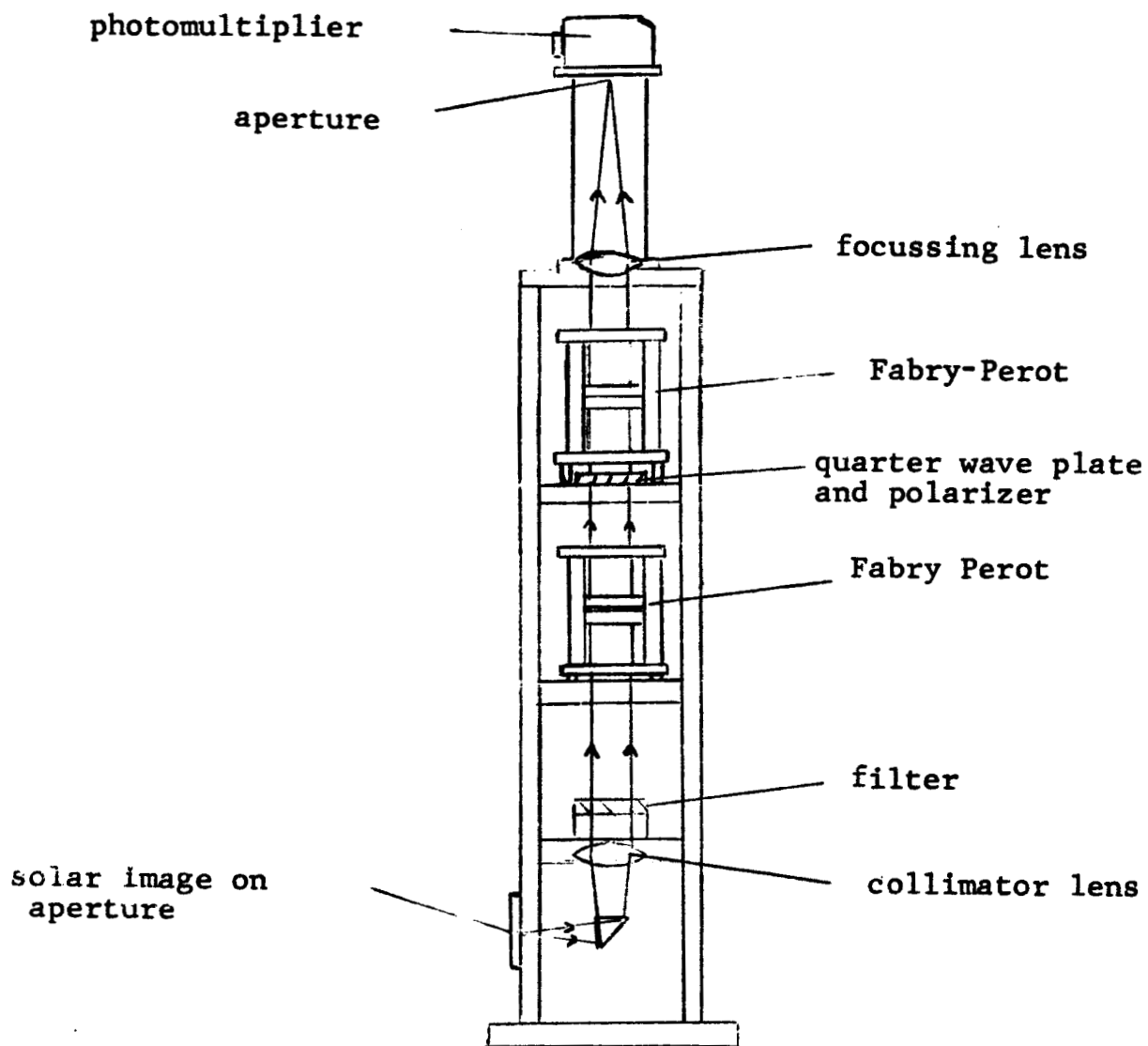


Figure 4. Showing present arrangement of two Fabry-Perot Interferometers in tandem

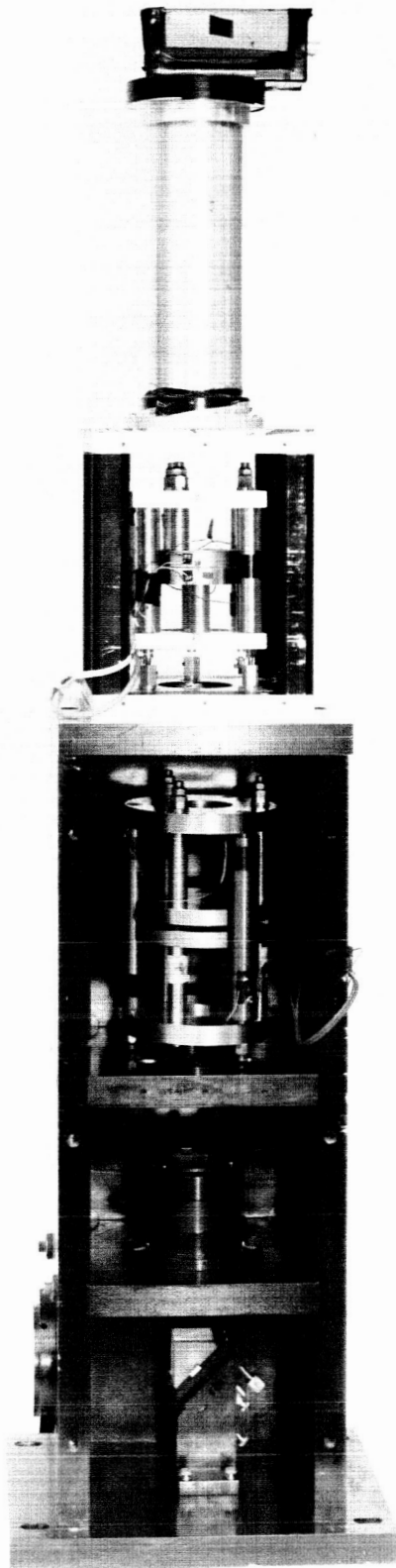


FIG. 5 PHOTOGRAPH OF BREADBOARD MODEL OF DOUBLE FABRY-PEROT SYSTEM.

continuum source such as a tungsten ribbon filament lamp. The tungsten lamp intensity distribution approximates that of a blackbody and, at a temperature of 2000°K , the intensity variation with wavelength of a blackbody is 0.01% per \AA at $\lambda 6500\text{\AA}$. Hence, over a 10\AA interval, the intensity of a tungsten lamp at about 3000°K may be regarded as constant to 0.1%. Fig. 9b shows the distribution of intensity transmitted by the monochromator. To achieve this form of transmission function, one of the slits of the scanning monochromator is made wider than the other. Figure 9c represents the multiple transmission function of the Fabry-Perot interferometer alone. Figure 9d shows the transmission function of the scanning monochromator-interferometer combination. As the monochromator and interferometer are scanned together the passbands keep in step on the wavelength so that, effectively, the spectrum is scanned by an instrument with a single narrow instrumental function as represented by Fig. 9d. Figures 10a and 10b show the various actual traces obtained using the bread-board model, a Keithley Model 417 picoammeter, and Moseley XY recorder. Figure 10a is a trace of the cadmium $\lambda 6438\text{\AA}$ emission line obtained from an Osram lamp. The discharge was focussed on the entrance slit of the monochromator and the Fabry-Perot scanned the line while the monochromator was kept fixed at the wavelength of the cadmium source, i.e., $\lambda 6438\text{\AA}$. The trace obtained was effectively the transmission function or instrumental profile of the Fabry-Perot since the line width of the cadmium emission line was negligible compared to the

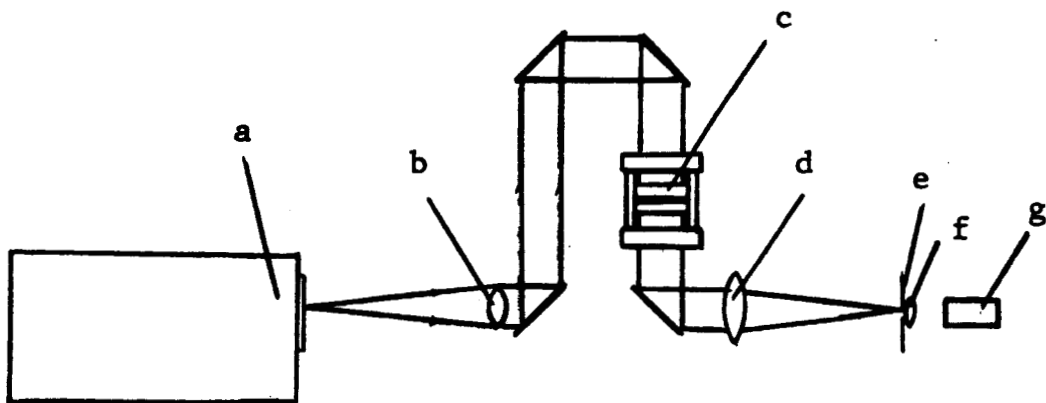


Fig. 6. Optical arrangement of synchronous scanning monochromator and Fabry-Perot interferometer.

- a) Scanning Monochromator
- b) Collimating Lens
- c) Fabry-Perot
- d) Focussing Lens
- e) Aperture Transmitting Central Order
- f) Field Lens
- g) Photomultiplier Tube.

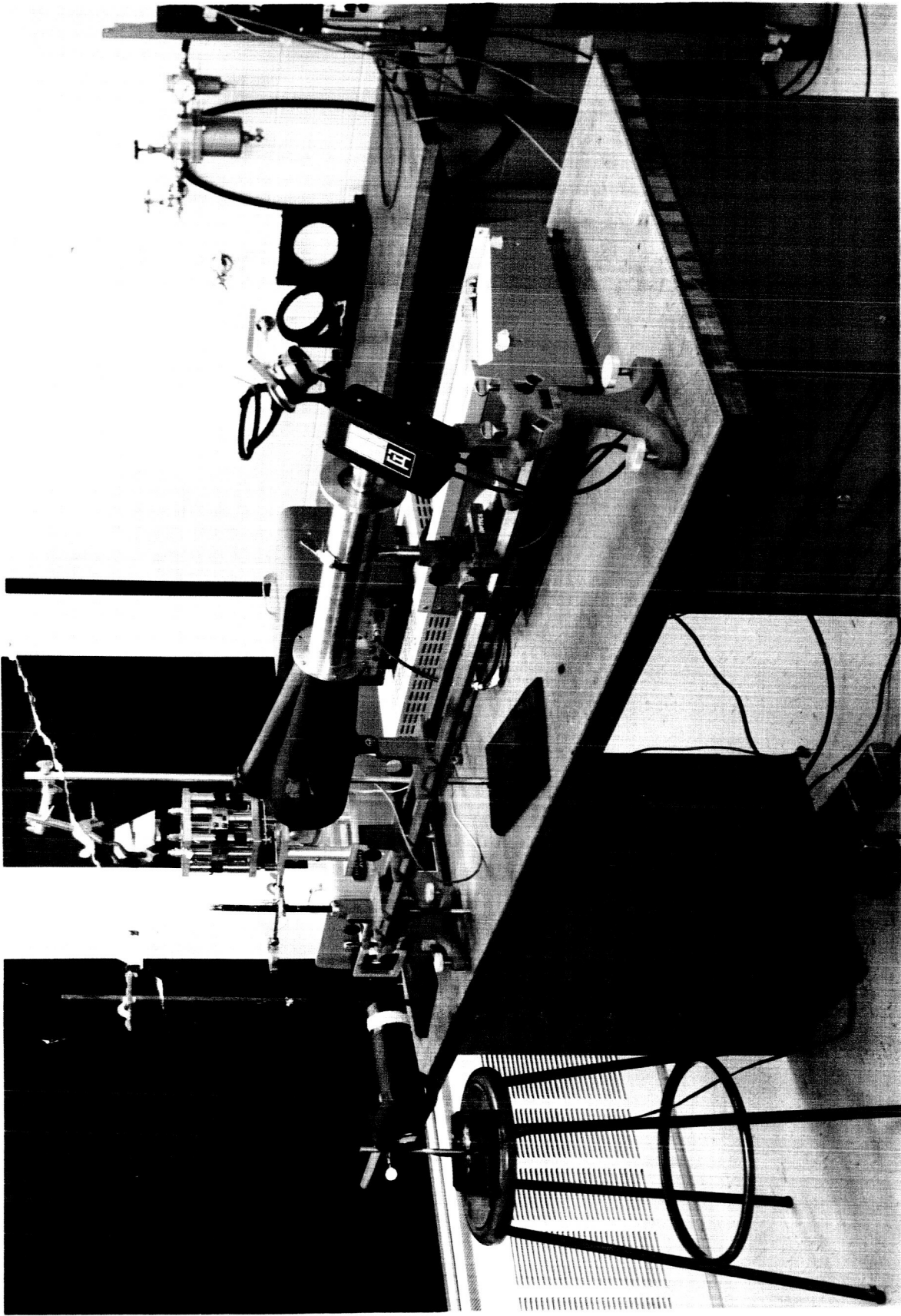


FIG. 7 PHOTOGRAPH OF BREADBOARD MODEL OF PRISM FABRY-PEROT AND MONOCHROMATOR

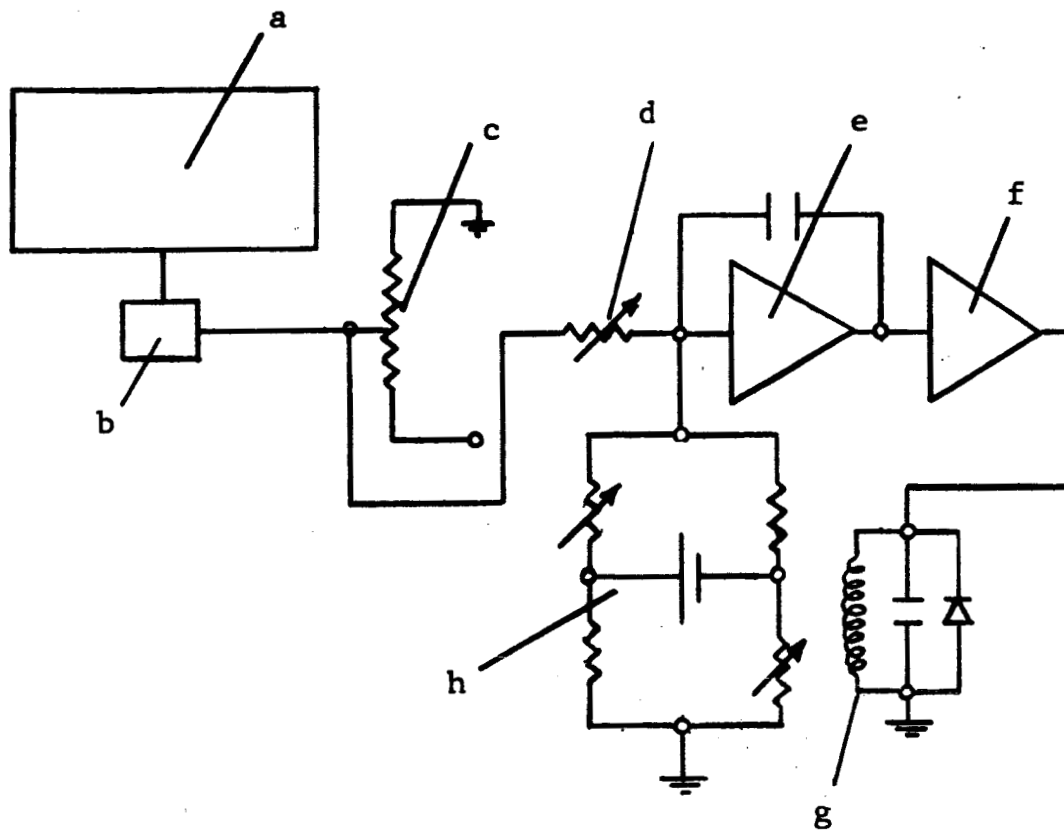
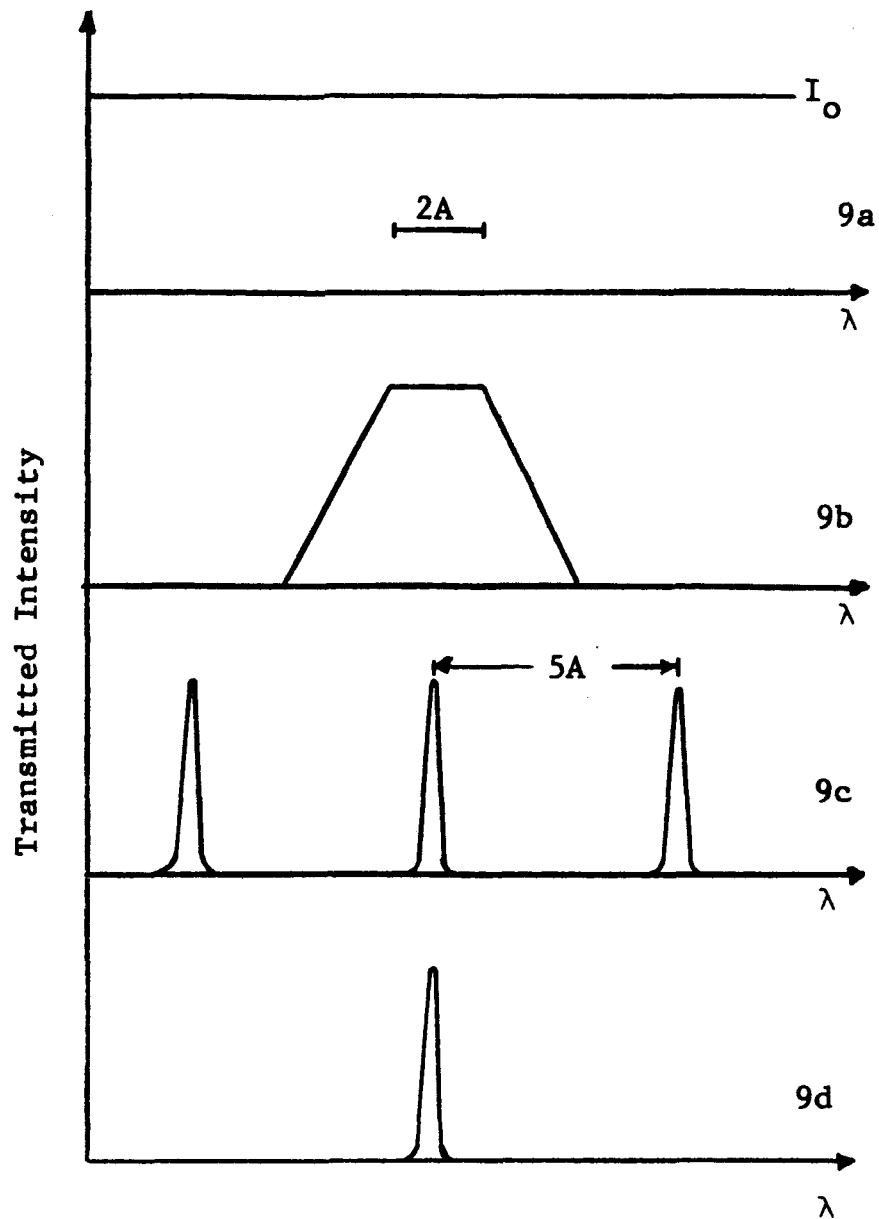


Fig.8. Block diagram of monochromator and interferometer scanning system.

- | | |
|--------------------------|-------------------------|
| a) Monochromator | g) Interferometer coils |
| b) Gear Train | h) Strain gage bridge |
| c) 10 turn Potentiometer | |
| d) Operational amplifier | |
| e) Operational amplifier | |
| f) Power amplifier | |



- Figure 9a Intensity distribution of tungsten ribbon filament lamp over short wavelength interval.
- Figure 9b Passband of monochromator operating at low resolution with mismatched entrance and exit slits.
- Figure 9c Passbands of Fabry-Perot interferometer
- Figure 9d Passband of monochromator and interferometer together.

instrumental profile. From Fig. 10a it can be seen that the finesse of the Fabry-Perot was 21 and, since the free spectral range was 5\AA , the instrumental function was, therefore, 0.24\AA . Fig. 10b shows a trace of the transmission function of the Jarrell-Ash Scanning Spectrometer used as a monochromator illuminated by a tungsten ribbon filament lamp and set at $\lambda 6438\text{\AA}$. The dispersion of the instrument was $64\text{\AA}/\text{mm}$, and matched entrance and exit slits of 24μ were used. The transmission function of the monochromator was then explored using the Fabry-Perot by holding the monochromator fixed at $\lambda 6438\text{\AA}$ and scanning the Fabry-Perot. Unfortunately, with the monochromator available, it was not possible to mismatch the entrance and exit slits in order to provide a flat-topped profile. The desirability of flattening the top of the profile of the monochromator is to relax the tolerance requirement on the synchronous scanning. This preliminary investigation was simply intended to test the feasibility of the system and so the lack of the flat-topped profile was not a hindrance at this stage.

The advantages to be gained by system (B) over, for instance, a simple grating spectrometer, may best be described in terms of the luminosity resolution product, $A\Omega R$, where A is the effective aperture, Ω is the solid angle of acceptance of system and R is the resolution of the instrument. Consider the half meter Ebert spectrometer used in the present program. The effective aperture, A , is the area of the grating and the solid angle of acceptance, Ω , is given by S/f^2 , where S is the

area of the entrance slit and f is the focal length of the collimating mirror. To obtain a given resolution with the spectrometer operating alone, a specific slit width is required and, hence, S is fixed. For example, the dispersion of the instrument, using a 300 grooves/mm grating, is $64\lambda/\text{mm}$ in the first order, and an instrumental function of 0.2λ requires a slit width of about 3μ . The value of 0.2λ used is, in fact, below the limit of resolution of the Jarrell-Ash instrument with this grating but, for the purpose of this comparison, this may be ignored. If now system (B) is used to obtain the same instrumental function, we can calculate the gain in luminosity over that given by the spectrometer alone. In system (B), the spectrometer operates at low resolution (i.e., larger slit width) as a monochromator. We may use the result obtained in Fig. 10B, which shows the instrumental profile of the monochromator for a slit width of 25μ , obtained with a resolution of slightly greater than 0.2λ . Since the area S and the luminosity are directly proportional to the slit width, system (B) represents a gain of slightly greater than 8 times in the luminosity for the same resolving power. The transmittance of the Fabry-Perot will probably reduce this value to about 7. It may be noted that the realization of this gain requires matching the Fabry-Perot optics to those of the monochromator in order to use all the light transmitted by the monochromator, i.e., the Fabry-Perot system will operate at $f/9$. We have therefore a significant

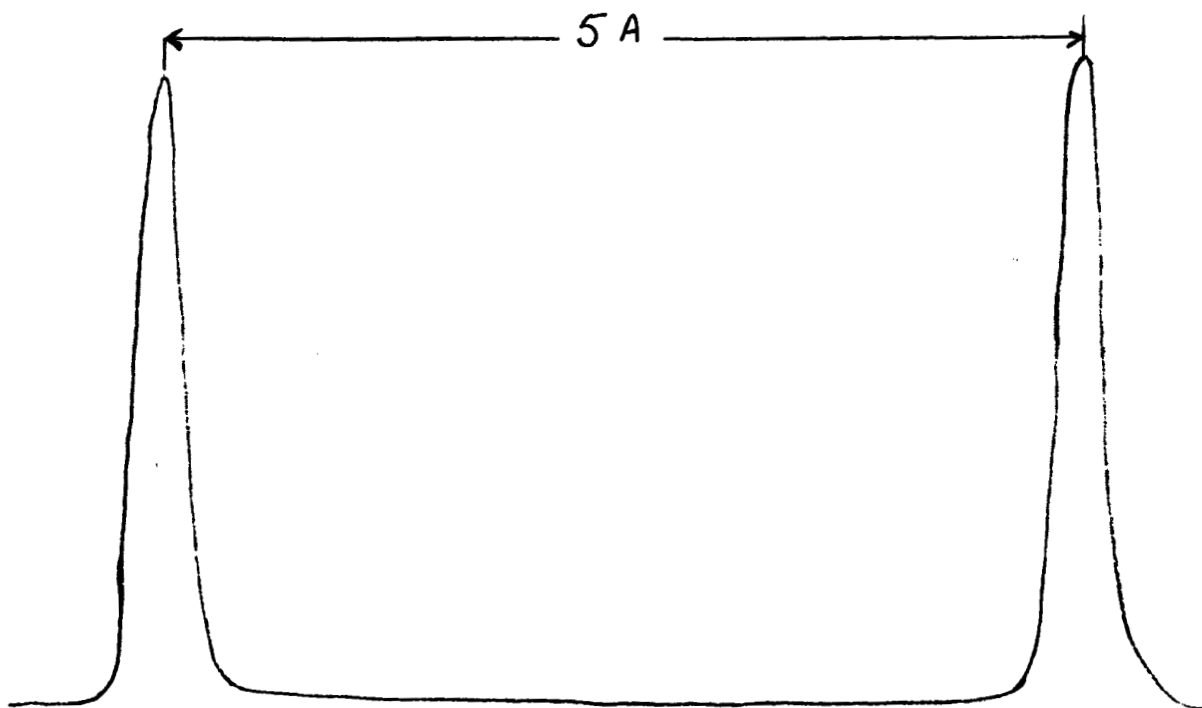


Fig. 10a. Trace obtained from cadmium lamp at $\lambda 6438 \text{ \AA}$ through monochromator and Fabry-Perot interferometer.

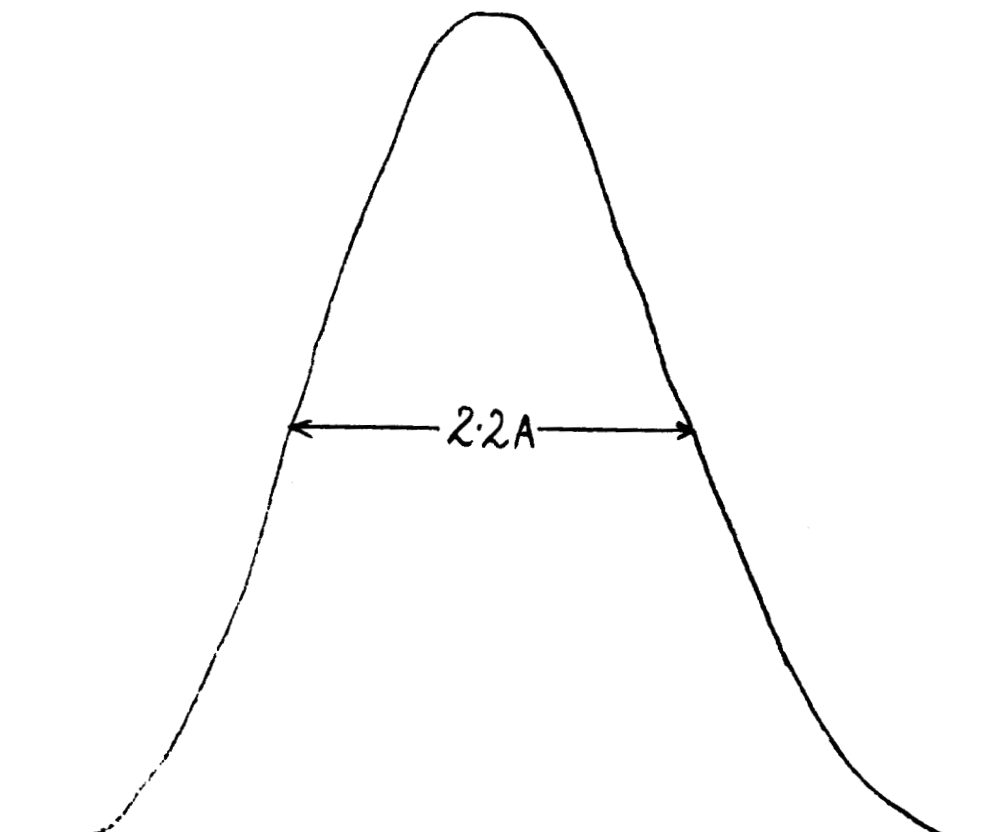


Fig. 10b. Trace of the instrumental function of the monochromator using the Fabry-Perot interferometer.

increase in the luminosity resolution product using the Fabry-Perot together with the monochromator.

Extending the above discussion to determine the gain of system (A) over (B), consider the optical system shown in Fig.4. The effective aperture A for this system is given by the useful aperture of the Fabry-Perot interferometer plates which is about 1/2 that of the grating in system (B).

The transmittance of the second interferometer will reduce the luminosity of system (A) by about 20% relative to (B).

The optimum solid angle subtended by the central order aperture of the scanning Fabry-Perot has been given by R. Chabbal (J. de Recherches du C.N.R.S. No. 24, 1953) and J. Jacquinot (Rep. Prog. Phys. p.267, 1960) as $2\pi R_o$, where R_o is the resolving power of the instrument.

$$R_o = \lambda / \sigma \lambda = \frac{6563}{0.2} = 32815.$$

Hence,

$$2\pi/R_o = \frac{2\pi}{32815} = 1.91 \times 10^{-4} \text{ ster.}$$

Due to the limb darkening of the sun it will be necessary to view only an area of the solar image limited to the central 10% of the solar diameter. Using a telescope of 178 cm focal length, an aperture of approximately 0.25 cm diameter is required to select the central 10% of the disc diameter. If the

IIT RESEARCH INSTITUTE

collimator in Fig. 4 has a focal length of 50 cm, then the solid angle subtended by the aperture is

$$\Omega = \frac{S}{f^2} = \frac{\pi(0.25)^2}{4 \times 50^2} = 1.94 \times 10^{-5} \text{ ster.}$$

The relevant solid angle for system (A) is the smaller of the two calculated, viz. 1.94×10^{-5} ster. System (B) has a solid angle of acceptance, Ω , given by the area of the slit in use. The slit width is 25μ and the height is 25 mm

$$\Omega = \frac{W \times H}{f^2} = \frac{0.0025 \times 0.25}{50^2} = 2.5 \times 10^{-7} \text{ ster.}$$

limited to the central 10% of the solar image diameter, i.e., 0.25 cm. We can now compare the luminosities of systems (B) and (A) thus:

$$\frac{(A\Omega)}{(A\Omega)} \frac{(A)}{(B)} = \frac{0.8}{1} \times \frac{1}{2} \times \frac{1.94 \times 10^{-5}}{2.5 \times 10^{-7}} = 31$$

The factor of 0.8 accounts for the additional transmission factor contributed by the second Fabry-Perot in (A). Hence, system (A) has a luminosity gain over (B) by a factor of about 30 times for a similar resolution.

Conclusions

The design considerations of a new method of attack on the problem of measuring the D/H ratio in the Solar photosphere have been investigated. Two feasible approaches have been investigated in detail, each capable, in principle, of fulfilling the requirements of the measurement. It is interesting to note that each of the systems investigated has general applications to high resolution spectroscopy in the field of astrophysics. For example, a system comprising a grating spectrograph and pressure scanned Fabry-Perot interferometer has been used by G. Münch at Mount Wilson Observatory. Dr. Münch is considering scanning the interferometer and spectrograph together. The interface problems associated with the pressure scanned interferometer should permit consideration of the magnetostrictive scanning system. The project leader will discuss this possibility with Dr. Münch in October 1966. The general applicability of a system of Fabry-Perot interferometers in series has been well demonstrated by the PEPSIOS instrument (Purely Interferometric High-Resolution Scanning Spectrometer) of the University of Wisconsin group. There is a case, however for a scanning system other than variation of pressure; since, due to adiabatic heating and the slow scan rates allowable with the pressure system, there is a limitation to its applicability.

Further development of the systems discussed in this report would be of benefit to observational astrophysics.

DISTRIBUTION LIST

<u>No. of Copies</u>	<u>Recipient</u>
25	Miss Winnie M. Morgan Technical Reports Officer Office of Grants and Research Contracts Office of Space Science and Applications National Aeronautics and Space Administration Washington, D. C. 20546
1	IIT Research Institute Schulz/Strohmeier/Main Files
1	IIT Research Institute J. J. Brophy
1	IIT Research Institute C. W. Terrell
1	IIT Research Institute B. A. Murray
3	IIT Research Institute Optics File

IIT RESEARCH INSTITUTE